

Nonlinear Characterization Techniques for Improving Accuracy of GaN HEMT Model Predictions in RF Power Amplifiers

Reinel Marante¹, José A. García¹, Lorena Cabria¹, Theophile Aballo¹, Pedro M. Cabral², José C. Pedro²

¹Dpto. Ingeniería de Comunicaciones, Universidad de Cantabria, 39005 Santander, SPAIN

²Instituto de Telecomunicações, Universidade de Aveiro, 3810-193, Aveiro, PORTUGAL

Abstract — In this paper, two vector nonlinear characterization procedures are presented, aimed at improving available GaN HEMT models for an accurate reproduction of the device behavior operating as a current source and in switched-mode RF power amplifiers (PAs). In the case of the more traditional linear amplifying classes, a technique for simultaneously extracting the higher order derivatives of the $I_{ds}(V_{gs})$, $I_{gs}(V_{gs})$ and $C_{gs}(V_{gs})$ transistor nonlinearities, along a desired load line, is described. This procedure conveniently isolates and models their contributions to the device intermodulation distortion (IMD) behavior. In the case of highly efficient switched-mode PAs, employed under drain modulation condition, a modified procedure for isodynamically measuring the higher order derivatives of the V_{dd} -to-AM and V_{dd} -to-PM amplifier profiles is put into consideration, as a way to refine the triode region reproduction for ON-OFF operation. The test set-ups, based on the combination of vector signal analysis and vector signal generation capabilities, are described in detail, together with some analytic expressions for the parameter extraction. Measured results for a 15 W device from Cree are finally included.

Index Terms — GaN HEMT, intermodulation distortion, linearity sweet-spots, nonlinear models, polar transmitters, power amplifiers.

I. INTRODUCTION

The solution to the spectral versus power efficiency tradeoff in multilevel or multicarrier wireless transmission is one of today's major concerns for the RF/microwave communities. Different linearization techniques, as predistortion or feedforward, have been developed along the last decades for traditional Cartesian (IQ) transmitters. More recently, special efforts are being directed to alternative topologies and, in particular, to polar architectures, where a theoretical 100% efficient operation would be possible thanks to the application of old high level AM strategies.

Device-level actions for linearity and efficiency optimization have become fundamental in modern PA conception, either in Cartesian or polar transmitters. Searching for linearity figures typical of small-signal operation at higher power levels and, consequently, improved associated efficiency values, class AB PA designers have been using self-linearization techniques, such as large-signal IMD sweet-spots [1]. On the other hand, actions at the transistor level may help understanding and controlling the nonlinearities that appear in drain modulated class E or F PAs [2].

Most of the available nonlinear device models fail in reproducing the device distortion performance in both operation modes, making a linear and efficient device-based PA design extremely difficult, or, at least, highly dependent on fine post-implementation adjustments. With the aim at solving such problems, and with the irruption in the wireless scenario of the promising GaN HEMT technology, significant efforts have been recently put in the development of nonlinear equivalent circuit representations with improved IMD prediction capabilities. These were conceived for either voltage-controlled current source amplifiers [3], or for dedicated switch-type models intended for drain modulated ON-OFF operation [4], requiring the experimental extraction of specific distortion related nonlinearity parameters.

In this paper, two vector-based nonlinear characterization procedures are proposed. These are destined to improve available GaN HEMT models for an accurate device behavior reproduction when operated as current source or in drain modulated switched-mode RF PAs. First, a technique for extracting the higher order derivatives of the $I_{ds}(V_{gs})$, $I_{gs}(V_{gs})$ and $C_{gs}(V_{gs})$ transistor nonlinearities along an isodynamic load line, is described. The method is intended to conveniently isolate, and later control, their contributions to the device large-signal IMD behavior. Then, a procedure for measuring the higher order derivatives of the V_{dd} -to-AM and V_{dd} -to-PM profiles of a polar transmitter modulating stage, free of low frequency dispersion effects, is put into consideration, with the purpose of accurately defining the device behavior in strong power saturation and as a way to improve the reproduction of the triode region characteristics determining its performance as a switch.

II. ISODYNAMIC EXTRACTION OF DEVICE HIGHER ORDER DERIVATIVES

The origin of large-signal IMD sweet-spots was related in [1] to the interaction between small- and large-signal IMD contributions, determined by the bias point derivatives and the strong device nonlinearities (saturation to triode region transition, gate junction conduction or breakdown). A good reproduction of the P_{in} - P_{out} IMD characteristics requires, at least, an accurate prediction of the predominant $I_{ds}(V_{gs})$ nonlinearity derivatives up to the 3rd order - see Eq. (1a) - along the selected load line. When increasing frequency, however, the reactive $C_{gs}(V_{gs})$ input nonlinearity, expanded in

Taylor series, as in Eq. (1b), seems to also contribute to this behavior, slightly modifying the shape, or position, of the sweet-spots. Besides that, a good selection of the load impedance for maximized output power inevitably leads to a current compression close to the onset of gate junction conduction, reason why the secondary effect of this resistive input nonlinearity, $I_{gs}(V_{gs})$ in Eq. (1c), should be also taken into account.

$$I_{ds}(V_{gs}) = I_{DS}(V_{GS}) + G_{m1} \cdot v_{gs} + G_{m2} \cdot v_{gs}^2 + G_{m3} \cdot v_{gs}^3 + \dots \quad (1a)$$

$$Q_{gs}(V_{gs}) = Q_{GS}(V_{GS}) + C_{gs1} \cdot v_{gs} + C_{gs2} \cdot v_{gs}^2 + C_{gs3} \cdot v_{gs}^3 + \dots \quad (1b)$$

$$I_{gs}(V_{gs}) = I_{GS}(V_{GS}) + G_{gs1} \cdot v_{gs} + G_{gs2} \cdot v_{gs}^2 + G_{gs3} \cdot v_{gs}^3 + \dots \quad (1c)$$

Experimental procedures, developed in the 90's [5, 6], allowed the extraction of the I_{ds} and C_{gs} derivatives, oriented to describe their IMD contribution, in FET small-signal operating conditions. However, when trying to address high power device characterization, the case of GaN HEMTs, for large-signal class A, AB, B or C operation, isodynamic, or pulsed measuring procedures, should be conceived as a way of avoiding undesired contributions from traps and self-heating effects.

A. Test Set-up for the Isodynamic Characterization of Generated Harmonic Content

In Fig. 1, a diagram of the proposed test set-up for input and output harmonic measurements, under pulsed conditions, is presented. Following the procedures presented in [5, 6], the excitation and the generated 2nd and 3rd harmonics are conveniently processed to reduce the nonidealities impact on the employed characterization hardware. To circumvent transistor low frequency dispersion effects, a short triangle-shape pulsed signal, able to sweep V_{gs} in 50 μ s and with a very low (0.1%) duty cycle, was inserted through the gate biasing path, and properly combined with a pulsed modulated 147 MHz RF excitation. The vector signal generators (Agilent ESG4438C) and vector signal analyzer (Agilent 89600) were digitally synchronized applying external trigger. Using the Distortion Suite application, the evolution with time of the input and output harmonics complex envelope was captured, to be employed in the derivatives extraction, as described in the next sub-section.

B. Volterra-series Derivative Extraction

After de-embedding the test set-up blocks response, the measured voltage envelopes allow calculating the corresponding gate and drain current components. In Fig. 2, a simplified GaN HEMT equivalent circuit schematic, corresponding to the employed characterization conditions, is shown. Due to the use of a pulsed excitation, the low frequency RC networks, describing dispersion, may be neglected. The value of the selected RF frequency also allows

avoiding contributions from reactive parasitics due to metallization, bonding, interelectrode capacitances, etc.

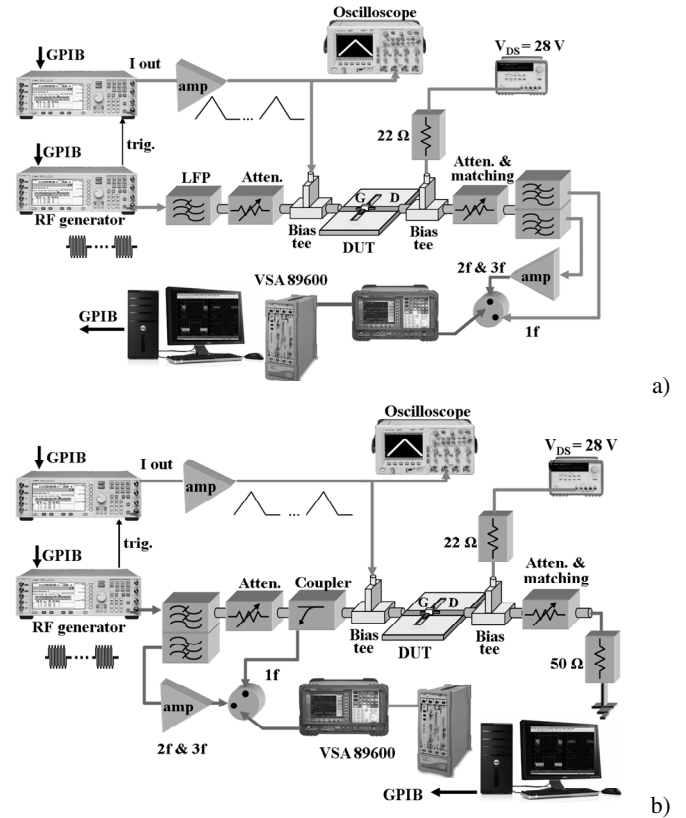


Fig. 1. Test set-up for a) output and b) input harmonic content measurements under isodynamic conditions.

Using Volterra-series, closed form expressions for the 2nd and 3rd degree coefficients in the Taylor-series expansions of Eq. (1) may be deduced. For simplicity, only the equations for G_{m2} , G_{gs2} and C_{gs2} are included in this paper.

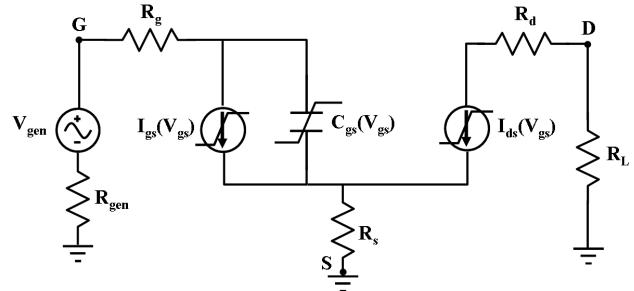


Fig. 2. Simplified GaN HEMT equivalent circuit.

$$G_{m2} = \frac{\text{Re} \left\{ \frac{2I_{ds}(2\omega) \cdot \text{Den}_2}{V_{gen}^2} \right\} (1 + G_{m1} R_s)}{\text{Den}_1} + \frac{\text{Re} \left\{ \frac{2I_{gs}(2\omega) \cdot \text{Den}_2}{V_{gen}^2} \right\} G_{m1} (R_{gen} + R_g + R_s)}{\text{Den}_1} \quad (2a)$$

$$G_{gs_2} = \frac{\operatorname{Re}\left\{\frac{2I_{gs}(2\omega) \cdot \text{Den}_2}{V_{gen}^2}\right\} [1 + G_{gs_1}(R_{gen} + R_g + R_s)]}{\text{Den}_1} + \quad (2b)$$

$$\frac{\operatorname{Re}\left\{\frac{2I_{ds}(2\omega) \cdot \text{Den}_2}{V_{gen}^2}\right\} G_{gs_1} R_s}{\text{Den}_1}$$

$$C_{gs_2} = \frac{1}{2\omega} \left[\operatorname{Im}\left\{\frac{2I_{gs}(2\omega) \cdot \text{Den}_2}{V_{gen}^2}\right\} + \quad (2c)$$

$$\operatorname{Im}\left\{\frac{2I_{ds}(2\omega)}{V_{gen}^2}\right\} \frac{R_s}{(R_{gen} + R_g + R_s)} \right]$$

$$\text{with } \text{Den}_1 = 1 + G_{m1}R_s + G_{gs1}(R_{gen} + R_g + R_s) \quad (2d)$$

$$\text{Den}_2 = [1 + (G_{gs1} + j\omega C_{gs1})(R_{gen} + R_g + R_s) + G_{m1}R_s]^2 \cdot [1 + (C_{gs1} + j\omega C_{gs1})(R_{gen} + R_g + R_s) + G_{m1}R_s] \quad (2e)$$

As it could be expected, the derivatives extraction for the input nonlinearities would only be possible if the input harmonic content were available as a vector magnitude, reason why the small-signal procedure in [6], based on scalar spectrum analyzer measurements, would not allow resolving input parameters.

In Fig. 3, the extracted results for a CGH35015 GaN HEMT from Cree Inc., along the optimum 22 Ω load line, are presented. The transconductance derivatives show significant values in the pinch-off and current compression regions, with asymmetric lobes to be considered in the nonlinear model extraction. The input diode nonlinearity contributes at high V_{gs} voltages, and the input capacitance shows a remarkable variation around pinch-off voltage (also observed in [6]) and in the onset of gate junction conduction, where the gate voltage control, over the channel charge, nearly disappears.

III. PULSED EXTRACTION OF A DRAIN MODULATED SWITCHING STAGE HIGHER ORDER NONLINEARITIES

A first procedure for extracting the higher order derivatives of the V_{dd} -to-AM and V_{dd} -to-PM nonlinearities in Eq. (3), for a switched mode PA, was proposed by the authors in [7].

$$AM(V_{dd}) = AM_0(V_{DD}) + m_1 \cdot v_{dd} + m_2 \cdot v_{dd}^2 + m_3 \cdot v_{dd}^3 + \dots \quad (3a)$$

$$PM(V_{dd}) = PM_0(V_{DD}) + p_1 \cdot v_{dd} + p_2 \cdot v_{dd}^2 + p_3 \cdot v_{dd}^3 + \dots \quad (3b)$$

A low frequency tone was added to the drain bias voltage, and the complex output envelope captured with the aid of a vector signal analyzer (VSA). However, the employed point to point characterization may be sensitive to low frequency dispersion mechanisms, mainly self-heating, reason why a small part of the observed amplitude compression at high

voltage values could be associated to a variation in the device channel temperature, during the measurement process.

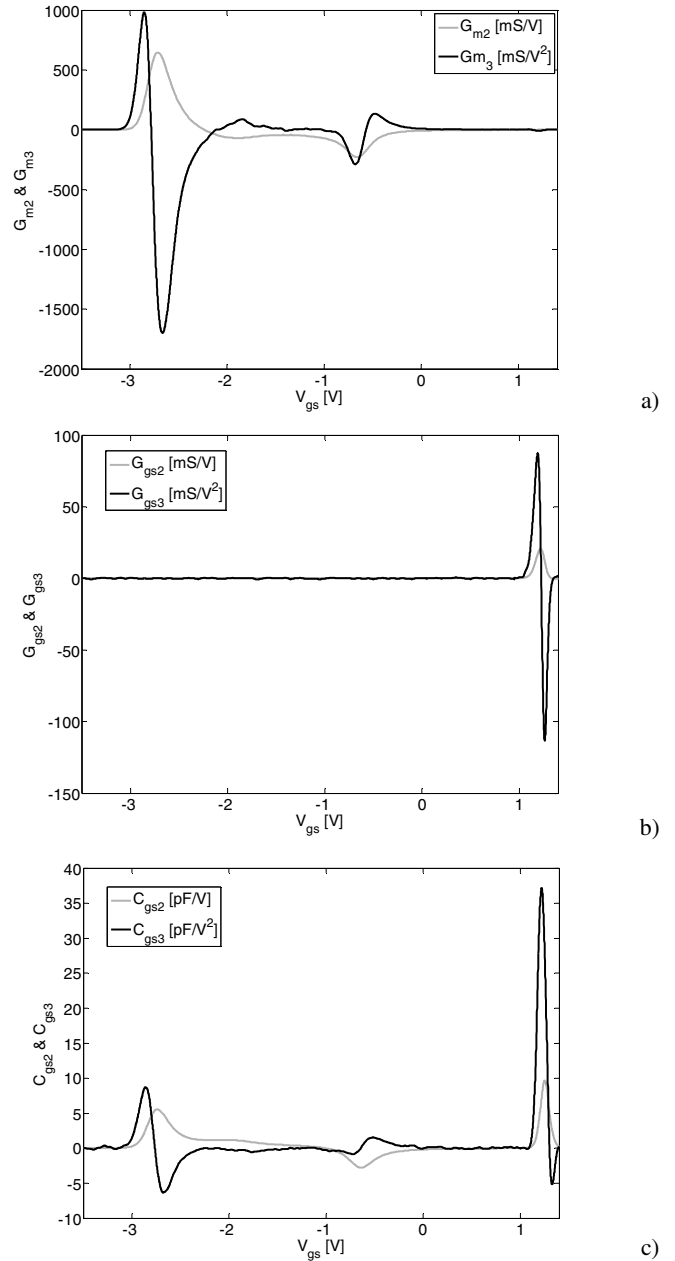


Fig. 3. Extracted GaN HEMT second and third order derivatives.

In Fig. 4, a diagram of the modified test set-up, now employing an isodynamic pulsed characterization, is presented. In this case, and due to the necessity of capturing the RF PA output time domain waveform, an adjustable pulsed voltage was inserted through the drain biasing path. The pulse-modulated low frequency tone was synchronized and added to the biasing pulse, thanks to the available digital delay control on the externally triggered mode of ESG vector signal generators. The 89600 vector signal analyzer was also

triggered, and the Distortion Suite used to capture the desired amplitude and phase components.

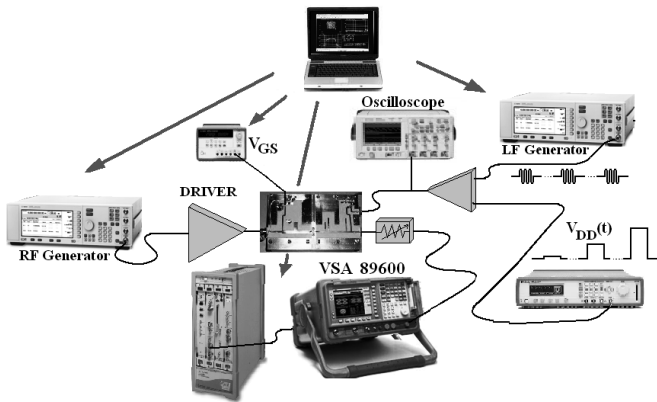


Fig. 4. Test set-up for output envelope measurements.

In Fig. 5, results of the extracted derivatives for a transmission line class E topology, based on the CGH35015 GaN HEMT, are finally shown. No noticeable contributions from kink effects to the modulating profiles have been detected. The observed low and high voltage nonlinearities follow the behavior predicted with the model in [2], reason why these derivatives could be used to accurately fit the R_{ON} and C_{gd} parameters.

IV. CONCLUSION

In this paper, two vector-based nonlinearity characterization procedures have been presented, aimed to improve available GaN HEMT models for an accurate reproduction of the device behavior operating as current source or in drain modulated switched-mode RF power amplifiers. The test set-ups employed for the isodynamic extraction of the device or circuit nonlinearity derivatives, based on the combination of vector signal analysis and vector signal generation capabilities, have been described to be decisive for accurate parameter extraction. Measured results for a CGH35015 GaN HEMT from Cree and a class E PA, designed over it, have been included for validation.

ACKNOWLEDGEMENT

This work was supported by the Spanish Ministerio de Ciencia e Innovación through projects TEC2008-06684-C03-01 and CSD2008-00068, as well as by the Portuguese Science Foundation, F.C.T., and Instituto de Telecomunicações under projects PTDC/EEA-TEL/65988/2006 Digital_PAs and SWIPA Ref. Nr.: P423, respectively. The authors also want to thank Ryan Baker, Cree Inc., by his kind assistance.

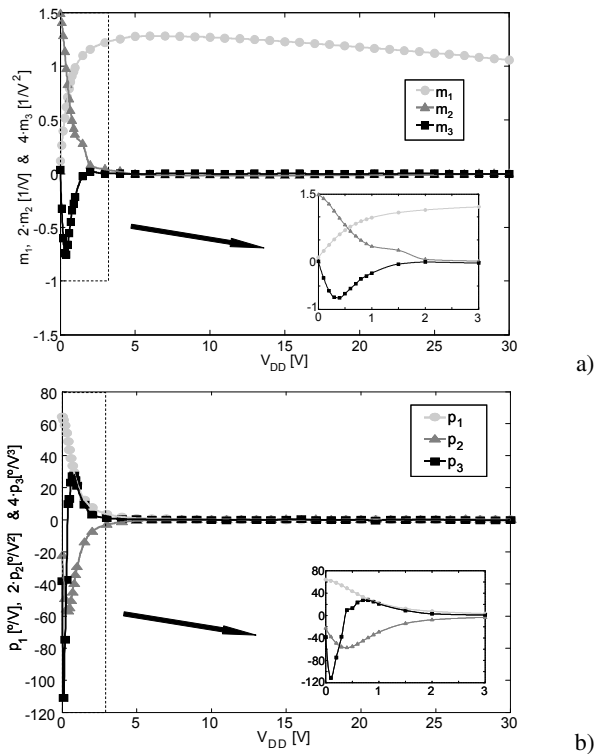


Fig. 5. Extracted V_{dd} -to-AM and V_{dd} -to-PM Taylor coefficients.

REFERENCES

- [1] N. Carvalho and J. Pedro, "Large and Small Signal IMD Behavior of Microwave Power Amplifiers", *IEEE Trans. Microwave Theory and Tech.*, vol. MTT-47, pp. 2364-2374, Dec. 1999.
- [2] J. C. Pedro, J. A. García and P. M. Cabral, "Nonlinear Distortion Analysis of Polar Transmitters," *IEEE Trans. Microwave Theory and Tech.*, vol. 55, no. 12, part 2, pp. 2757-2765, Dec. 2007.
- [3] P. M. Cabral, J. C. Pedro and N. B. Carvalho, "Nonlinear Device Model of Microwave Power GaN HEMTs for High-Power Amplifier Design", *IEEE Trans. Microwave Theory and Tech.*, vol. 52, no. 11, pp. 2585-2592, Nov. 2004.
- [4] P. Aflaki, R. Negra and F. Ghannouchi, "Dedicated Large-Signal GaN HEMT Model for Switching-Mode Circuit Analysis and Design," *IEEE Microwave and Wireless Components Letters*, vol. 19, no. 11, pp. 740-742, Nov. 2009.
- [5] J. C. Pedro, and J. Perez, "Accurate Simulation of GaAs MESFET's Intermodulation Distortion Using a New Drain-Source Current Model," *IEEE Trans. Microwave Theory Tech.*, vol. 42, no.1, pp. 25-33, Jan. 1994.
- [6] J. A. García, A. Mediavilla, J. C. Pedro, N. B. Carvalho, A. Tazón, and J. L. García, "Characterizing the Gate-to-Source Nonlinear Capacitor Role on GaAs Fet IMD Performance", in *IEEE Trans. Microwave Theory and Tech.*, vol. 46, no. 12, pp. 2344-2355, Dec. 1998.
- [7] J. A. García, B. Bedia, R. Merlín, P. M. Cabral and J. C. Pedro, "Characterizing the V_{dd} -to-AM and V_{dd} -to-PM Nonlinearities in a GaN HEMT Class E Power Amplifier", *Proc. International Symp. on Microwave and Optical Technology - ISMOT*, Rome, Italy, pp. 375 - 378, December, 2007.